

# Distributed Event-triggered Secondary Control for Average Bus Voltage Regulation and Proportional Load Sharing of DC Microgrid

Zhongwen Li, Zhiping Cheng, Jikai Si, and Shuhui Li

**Abstract**—This paper proposes a novel distributed event-triggered secondary control method to overcome the drawbacks of primary control for direct current (DC) microgrids. With event-triggered distributed communication, the proposed control method can achieve system-wide control of parallel distributed generators (DGs) with two main control objectives: ① estimate the average bus voltage and regulate it at the nominal value; ② achieve accurate current sharing among the DGs in proportion to their power output ratings. Furthermore, the proposed control strategy can be implemented in a distributed way that shares the required tasks among the DGs. Thus, it shows the advantages of being flexible and scalable. Furthermore, this paper proposes a simple event-triggered condition that does not need extra state estimator. Thus, limited communication among neighbors is required only when the event-triggered condition is satisfied, which significantly reduces the communication burden at the cyber layer.

**Index Terms**—Direct current (DC) microgrid, droop control, event-triggered secondary control, distributed consensus, load sharing.

## I. INTRODUCTION

RECENTLY, direct current (DC) microgrids have received increasing attention due to major superiorities over alternating current (AC) microgrids such as higher efficiency and reliability [1]. DC power sources and storage systems such as solar photovoltaic (PV) arrays, fuel cells, and batteries, can be integrated into the DC microgrid without the need of additional AC/DC or DC/AC converters. Furthermore, another advantage of a DC microgrid is the lack of problems related to reactive power and frequency regulations.

For a DC microgrid, a voltage-current droop control method is generally applied in the primary-level control, which

can regulate the output power of a dispatchable distributed generator (DG) based on its terminal voltage variation [2], [3]. Although the primary droop control can increase the voltage stability and reduce the circulating current between parallel DGs [4], there are certain drawbacks in conventional droop control [5]. Firstly, it shows steady-state DC bus deviation due to the voltage drop. Secondly, it shows inaccurate current sharing due to unbalanced line resistances. To overcome the drawbacks of the primary droop control, a secondary control is generally required to restore voltage deviation and improve current sharing [6].

In recent years, some centralized secondary control approaches have been applied to regulate bus voltage of a DC microgrid [4], [7]. However, a central controller is generally required to execute the communication and computation tasks that are needed for the secondary control, which is inflexible and susceptible to single-point failure [8]. Furthermore, with a distributed control method, the complex and necessary communication and computing tasks can be shared among each DG through parallel processing. Thus, the distributed control methods show the advantages of being flexible, scalable, and robust against single-point failure.

Due to the advantages of distributed control strategies, several distributed secondary control strategies have been studied for current sharing and/or voltage regulation of DC microgrids [9]-[15]. These include a distributed strategy to achieve current sharing among the DGs in a DC microgrid [9], a secondary voltage control method to regulate the bus voltage to its nominal value for a droop-controlled DC microgrids [10], a communication-based secondary control strategy for current sharing and voltage regulation of a DC microgrid [11], a voltage-shifting and slope-adjusting based secondary control scheme to improve the droop control of DC microgrids [12], a distributed optimal control scheme to realize proportional load sharing and voltage regulation functions through tuning the weighting coefficients between the two functions [13], and a consensus-based secondary control for voltage regulation and current sharing of a DC microgrid [14], [15]. However, all these methods [9]-[15] are implemented based on a time-triggered communication strategy, which needs communication among neighboring agents in a periodic time interval. Thus, the communication burden will greatly increase, especially when the microgrid is expanded with more DGs. Furthermore, most of these methods [9]-[11], [15] typically require global communication to acquire

Manuscript received: November 3, 2020; revised: March 1, 2021; accepted: June 10, 2021. Date of CrossCheck: June 10, 2021. Date of online publication: July 14, 2021.

This work was supported by the National Natural Science Foundation of China (No. 61803343) and Key R&D and Promotion Project of Henan Province (No. 202102210096).

This article is distributed under the terms of the Creative Commons Attribution 4.0 International License (<http://creativecommons.org/licenses/by/4.0/>).

Z. Li, Z. Cheng (corresponding author), and J. Si are with the School of Electrical Engineering, Zhengzhou University, Zhengzhou 450001, China (e-mail: lzw@zzu.edu.cn; zpcheng@zzu.edu.cn; sijikai@zzu.edu.cn).

S. Li is with the Department of Electrical and Computer Engineering, The University of Alabama, Tuscaloosa, AL 35487, USA (e-mail: sli@eng.ua.edu).

DOI: 10.35833/MPCE.2020.000780



information from all other agents for those distributed current sharing control methods to work properly. This paper intends to design a distributed and event-triggered secondary control method for current sharing and voltage regulation of a DC microgrid so as to significantly reduce the communication burden and to develop a current sharing strategy that is only based on the local current measurement and minimum current information from a few neighbors' current information, which is easy to implement.

Recently, several event-triggered control methods [16] - [20] have been studied and developed. In [16], [17], adaptive event-triggered secondary control strategies are proposed for average voltage regulation as well as proportional load sharing. However, both current and voltage estimators are required to generate an event-triggered condition, which is complex to implement. In [18], an event-triggered distributed nonlinear control strategy is studied to improve current-sharing as well as voltage regulation for a DC microgrid. However, it only focuses on regulating output voltage around the nominal value, and thus shows steady-state voltage deviation between average bus voltage and its nominal value. In [19], an event-triggered discrete-time control method is studied for both bus voltage and current sharing control of a DC microgrid. However, the initial average bus voltage is assumed to be equal to the nominal value, and the Laplacian matrices of the electrical and communication networks are assumed to be commutative [19], which restricts its flexibility and expandability. In [20], an event-triggered distributed method is proposed to improve voltage restoration and current sharing of a DC microgrid. For the methods proposed in [19], [20], several parameters and a positive definite matrix need to be well designed for the event-triggered condition. Different from the methods shown in [16], [17], [19], [20], the proposed method of this paper, as detailed in Section IV, requires only one parameter to be designed based upon the proposed event-triggered condition. The proposed method does not need extra state estimators and has a low computational burden, which is easier to implement.

The primary contributions of this paper include: ① a novel method for simultaneous average bus voltage restoration and proportional load sharing of a DC microgrid in the proposed secondary control level that requires only local current measurement and information from the corresponding neighbors; ② an event-triggered mechanism to significantly reduce the communication burden that does not need additional state estimators or complex parameter design to decide the event-triggered condition and thus easy to implement; ③ detailed convergence analysis and integrated simulation study of a DC microgrid that contains multiple control levels to verify the performance of the proposed control strategy under over-load, plug-and-play, and agent-loss conditions.

The remainder of this paper is organized as follows. The background preliminary is presented in Section II. The distributed secondary control is presented in Section III. The event-triggered implementation of the proposed secondary control is presented in Section IV. In Section V, simulation verification and result analysis are provided. Finally, conclu-

sions are presented in Section VI.

## II. BACKGROUND PRELIMINARY

### A. Graph Theory

Generally, graph theory is widely applied to model the communication topology of a network of distributed agents [21], [22]. In order to model the distributed communication between agents as a graph, each agent is represented by a node, and the communication links between agents are represented by edges [22]. A graph is generally defined as  $G = (V, E)$ , where  $V = \{1, 2, \dots, n\}$  is a set of nodes,  $n$  is the number of nodes in the graph; and  $E \subseteq V \times V$  is a set of edges. The set of the neighboring agents of the  $i^{\text{th}}$  node can be defined as  $N_i = \{j \in V \mid (i, j) \in E\}$ .

### B. Distributed Consensus Theory

Based on the graph theory, a matrix  $\mathbf{W} \in \mathbf{R}^{n \times n}$  is referred to an Laplacian matrix [23] of graph  $G$  if its elements  $w_{i,j}$  is calculated based on the following equation.

$$w_{i,j} = \begin{cases} -\frac{1}{n_i + n_j + \zeta} & \text{agents } i \text{ and } j \text{ are connected} \\ \sum_{j \in N_i} \frac{1}{n_i + n_j + \zeta} & \text{for diagonal elements} \\ 0 & \text{agents } i \text{ and } j \text{ are disconnected} \end{cases} \quad (1)$$

where  $n_i$  and  $n_j$  are the numbers of neighbors of the  $i^{\text{th}}$  and  $j^{\text{th}}$  agents, respectively; and  $\zeta$  is a real number for regulating eigenvalues of matrix  $\mathbf{W}$ .

Based on the definition of  $w_{i,j}$  shown in (1), we can infer that matrix  $\mathbf{W}$  is positive semi-definite and symmetric.

According to [24], [25], a distributed consensus algorithm could be represented by the following linear system.

$$\dot{\mathbf{x}}(t) = -\varepsilon \mathbf{W} \mathbf{x}(t) \quad (2)$$

where  $\varepsilon$  is a gain factor to regulate convergence speed of the distributed consensus method; and  $\mathbf{x}(t) \in \mathbf{R}^{n \times 1}$  is the system state at time  $t$ .

According to the distributed consensus theory, if a consensus is reached, the system state will converge to the average value of all agents' initial state [24]. Thus, the convergence state is:

$$\lim_{t \rightarrow \infty} \mathbf{x}(t) = \frac{1}{n} \mathbf{\Phi} \mathbf{x}(0) \quad (3)$$

where  $\mathbf{\Phi} \in \mathbf{R}^{n \times n}$  is a square matrix and all its elements equal to 1; and  $\mathbf{x}(0)$  is the initial system state.

Based on the distributed consensus theory and the definition of  $\mathbf{W}$ , the following properties can be derived.

Property 1: if  $\mathbf{W}$  is a Laplacian matrix defined as (1), then the following equation will be satisfied:

$$\lim_{s \rightarrow 0} s(s\mathbf{I} + \varepsilon \mathbf{W})^{-1} = \frac{1}{n} \mathbf{\Phi} \quad (4)$$

where  $\mathbf{I}$  is a unity matrix.

Proof: the Laplace transform of  $\mathbf{x}(t)$  is represented by  $\mathbf{X}(s)$ , then the Laplace transform of linear system shown in (2) can be presented in the  $s$ -plane as follows:

$$\mathbf{X}(s) = (s\mathbf{I} + \varepsilon\mathbf{W})^{-1} \mathbf{x}(0) \quad (5)$$

According to the final value theorem of Laplace transform, we have:

$$\lim_{t \rightarrow \infty} \mathbf{x}(t) = \mathbf{x}^{ss} = \lim_{s \rightarrow 0} s(\mathbf{I} + \mathbf{W})^{-1} \mathbf{x}(0) \quad (6)$$

where  $\mathbf{x}^{ss}$  is the steady-state system state.

Comparing (3) and (6), we can infer that (7) is satisfied.

$$\lim_{s \rightarrow 0} s(\mathbf{I} + \mathbf{W})^{-1} \mathbf{x}(0) = \frac{1}{n} \Phi \mathbf{x}(0) \quad (7)$$

As (7) is always satisfied for  $\mathbf{x}(0) \neq \mathbf{0}$ , Property 1 shown in (4) is also satisfied.

Property 2: define  $b$  as a constant real number, and  $\mathbf{1} = [1, 1, \dots, 1]^T \in \mathbf{R}^{n \times 1}$ , if the linear equation (8) is solvable, then we can infer that  $b=0$ , and the solution of linear equation presented in (8) can be represented by  $\mathbf{x} = \gamma \mathbf{1}$ , which means each element of  $\mathbf{x}$  converges to a common value.

$$\mathbf{W}\mathbf{x} = b\mathbf{1} \quad (8)$$

Proof: according to the definition of Laplacian matrix  $\mathbf{W}$  shown in (1), we can infer that the summations of all the row elements of  $\mathbf{W}$  are equal to zero. Thus, we can infer that zero is one eigenvalue of matrix  $\mathbf{W}$  and that the corresponding eigenvector is  $\mathbf{1} = [1, 1, \dots, 1]^T$ . If graph  $G$  is strongly connected, then  $\text{rank}(\mathbf{W}) = n - 1$  [25].

Based on the consistency theory [26], [27], if the linear equation (8) is solvable, (9) will be satisfied.

$$\text{rank}(\mathbf{W}) = \text{rank}([\mathbf{W}, b\mathbf{1}]) = n - 1 \quad (9)$$

According to (9), we can infer that  $b=0$ . As the matrix  $\mathbf{W}$  has an eigenvalue of zero and eigenvector  $\mathbf{1} = [1, 1, \dots, 1]^T$ , the general solution of homogeneous system  $\mathbf{W}\mathbf{x} = \mathbf{0}$  has the following form [26]:

$$\mathbf{x} = \gamma [1, 1, \dots, 1]^T = \gamma \mathbf{1} \quad (10)$$

Thus, based on the above analysis, Property 2 is satisfied.

### III. DISTRIBUTED SECONDARY CONTROL

Figure 1 presents the hierarchical control architecture of a DC microgrid, which includes a primary droop control and a proposed distributed secondary control, where PWM represents pulse width modulation.

In this section, the control objective of proposed distributed secondary control is firstly presented to overcome the drawbacks of primary droop control. Secondly, the distributed average bus voltage discovery strategy is proposed and applied for the secondary voltage restoration control. The design process of the distributed secondary control algorithm is presented in the following subsections.

#### A. Control Objective

In order to ensure the primary load sharing between parallel DGs, the voltage-current droop control strategy is widely applied in the primary droop control of a DC microgrid [9], [11]. For a converter-interfaced DG, the voltage & current controllers can generate the appropriate output voltage reference for its inner-loop voltage controller as follows:

$$v_{ref,i}(t) = v_{nom} - m i_{pu,i}(t) \quad (11)$$

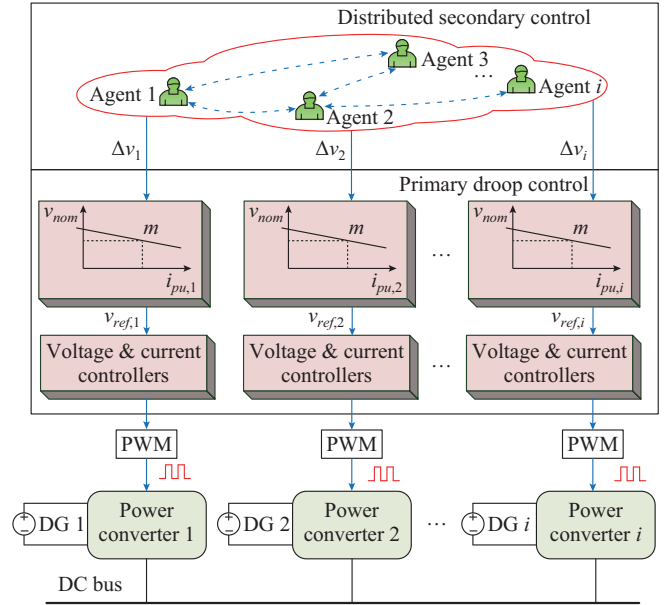


Fig. 1. Hierarchical control architecture of DC microgrid.

where  $v_{ref,i}(t)$  is the output voltage reference of inner-loop voltage controller for DG  $i$ ;  $v_{nom}$  is the nominal value of bus voltage;  $m$  is the droop coefficient; and  $i_{pu,i}(t)$  is the per-unit current output of DG  $i$  that can be calculated as:

$$i_{pu,i}(t) = \frac{i_i(t)}{i_{max,i}} \quad (12)$$

where  $i_i(t)$  and  $i_{max,i}$  are the current and the maximum current of DG  $i$ , respectively.

Generally, the larger the droop coefficient is, the more accurate the load sharing is, while the higher the voltage deviation will be. Thus, the primary droop control shows an inherent trade-off between voltage regulation and current sharing when several DGs operate in parallel [28], [29].

In order to overcome the drawbacks of primary droop control, a distributed event-triggered secondary control method is proposed to generate a voltage regulating term  $\Delta v_i(t)$  and improve the conventional droop control shown in (11) as:

$$v_{ref,i}(t) = v_{nom} - i_{pu,i}(t)m + \Delta v_i(t) \quad (13)$$

In this paper, the following control objectives are considered for the proposed secondary control strategy.

1) Restore the average bus voltage of a DC microgrid to the nominal value  $v_{nom}$  through adjusting voltage regulating term  $\Delta v_i(t)$  and shifting the conventional droop control through (13).

2) Achieve accurate current sharing between droop controlled DGs in proportion to their capacities by adjusting the voltage regulating term  $\Delta v_i(t)$  and shifting the conventional droop control through (13).

#### B. Distributed Average Bus Voltage Discovery

In order to restore the average bus voltage of a DC microgrid to its nominal value, the average bus voltage of the microgrid needs to be discovered first. Thus, based on the distributed consensus theory [23], [30], a distributed average bus voltage discovery algorithm is designed as shown in

(14), which can allow each DG agent to discover the average bus voltage of a DC microgrid based on distributed communication. After discovering the average bus voltage through (14), the average bus voltage can then be easily recovered later in Section III-C.

$$v_{ave,i}(t) = v_i(t) - \varepsilon \int_0^t \sum_{j \in \{i, N_i\}} w_{i,j} v_{ave,j}(\tau) d\tau \quad (14)$$

where  $v_{ave,i}(t)$  is the discovered average bus voltage hold by DG  $i$ ;  $v_i(t)$  is the measured output voltage of DG  $i$ ; and  $\varepsilon > 0$  is a gain factor, which can tune the convergence speed of distributed average bus voltage discovery algorithm.

Different from the dynamic consensus algorithm proposed in [31], [32], a gain factor  $\varepsilon > 0$  is added in the distributed average bus voltage discovery algorithm for the DC microgrid, as shown in (14). With the freely adjustable parameter  $\varepsilon$ , the convergence speed of the algorithm can be easily adjusted to a satisfactory value. In the following, the convergence of the algorithm shown in (14) is analyzed.

Define  $V_{ave,i}(s)$ ,  $V_i(s)$  as the Laplace transforms of  $v_{ave,i}(t)$ ,  $v_i(t)$ , respectively. Then, the Laplace transform of (14) is:

$$sV_{ave,i}(s) = -\varepsilon \sum_{j \in \{i, N_i\}} w_{i,j} V_{ave,j}(s) + sV_i(s) \quad (15)$$

Based on the definition of Laplacian matrix  $\mathbf{W}$  shown in (1), the compact form of (15) can be rewritten as:

$$s\mathbf{V}_{ave}(s) = -\varepsilon \mathbf{W} \mathbf{V}_{ave}(s) + s\mathbf{V}(s) \quad (16)$$

where  $\mathbf{V}_{ave}(s) = [V_{ave,1}(s), V_{ave,2}(s), \dots, V_{ave,n}(s)]^T$ ; and  $\mathbf{V}(s) = [V_1(s), V_2(s), \dots, V_n(s)]^T$ .

According to (16), the following equation can be derived:

$$\mathbf{V}_{ave}(s) = (s\mathbf{I} + \varepsilon \mathbf{W})^{-1} s\mathbf{V}(s) \quad (17)$$

Define  $\mathbf{v}_i^{ss}$  as the steady-state bus voltage of DG  $i$ , and  $\mathbf{v}^{ss} = [v_1^{ss}, v_2^{ss}, \dots, v_n^{ss}]^T$ , thus, according to the final value theory of Laplace transform, the following equation will be derived:

$$\mathbf{v}^{ss} = \lim_{s \rightarrow 0} s\mathbf{V}(s) \quad (18)$$

Then, according to the final value theory of Laplace transform, and by substituting (4) and (18) into (17), the following equation can be derived:

$$\mathbf{v}_{ave}^{ss} = \lim_{t \rightarrow \infty} \mathbf{v}_{ave}(t) = \lim_{s \rightarrow 0} s\mathbf{V}_{ave}(s) = \lim_{s \rightarrow 0} s(s\mathbf{I} + \varepsilon \mathbf{W})^{-1} s\mathbf{V}(s) = \frac{1}{n} \Phi \mathbf{v}^{ss} \quad (19)$$

As  $\Phi \in \mathbf{R}^{N \times N}$  is defined as a square matrix and all its elements equal to 1,  $\mathbf{v}_{ave,i}$  can converge to the corresponding average value of the voltages of all DGs for  $i = 1, 2, \dots, N$ .

### C. Distributed Secondary Control Algorithm Design

To satisfy these two control objectives presented in Section III-A, a distributed secondary control is proposed in this subsection, in which DG  $i$  generates the voltage regulating term  $\Delta v_i(t)$  by communicating with its neighboring DG agents in a distributed way based on the following equation.

$$\Delta v_i(t) = k_{pv} (v_{nom} - v_{ave,i}(t)) + k_{iv} \int_0^t (v_{nom} - v_{ave,i}(\tau)) d\tau - k_{pc} \sum_{j \in \{i, N_i\}} w_{i,j} i_{pu,j}(t) - k_{ic} \int_0^t \sum_{j \in \{i, N_i\}} w_{i,j} i_{pu,j}(\tau) d\tau \quad (20)$$

where  $k_{pv} > 0$  and  $k_{iv} > 0$  are the proportion and integral factors for voltage restoration, respectively, which affect the convergence speed of voltage restoration; and  $k_{pc} > 0$  and  $k_{ic} > 0$  are the proportion and integral factors for load sharing, which affect the convergence speed of proportional load sharing, respectively.

As shown in (20), only local current measurement and information from the corresponding neighboring agents are required to ensure the proportional current sharing, while the average current or circulating current of the DGs is not required. Thus, the proposed algorithm shown in (20) is different from the load sharing algorithms proposed in [14], [15]. In [14], the average circulating current needs to be obtained using a consensus algorithm before generating a modified droop control action, which is complex to implement. In [15], on the other hand, in order to generate an updated voltage control action, the per-unit output power of each DG needs to be identified through sharing information among all DGs via a low-bandwidth communication, which will increase the communication cost.

The distributed secondary control algorithm is converged and can satisfy these control objectives proposed in Section III-A as demonstrated in the following part.

Define  $\Delta V_i(s)$ ,  $V_{nom}(s) = v_{nom}/s$ , and  $I_{pu,i}(s)$  as the Laplace transforms of  $\Delta v_i(t)$ ,  $v_{nom}$ , and  $i_{pu,i}(t)$ , respectively. Then, the Laplace transform of (20) can be defined as:

$$s\Delta V_i(s) = (sk_{pv} + k_{iv}) \left( \frac{v_{nom}}{s} - V_{ave,i}(s) \right) - (sk_{pc} + k_{ic}) \sum_{j \in \{i, N_i\}} w_{i,j} I_{pu,j}(s) \quad (21)$$

Furthermore, define  $V_{ref,i}(s)$  as the Laplace transform of  $v_{ref,i}(t)$ . Thus, the Laplace transform of (13) can be defined as:

$$V_{ref,i}(s) = \frac{v_{nom}}{s} - I_{pu,i}(s)m + \Delta V_i(s) \quad (22)$$

Generally, the primary droop control and the inner voltage control loops show much higher response speed than the proposed secondary control [33]. Thus, we can assume that  $v_{ref,i}(t) = v_i(t)$ . Define  $V_i(s)$  as the Laplace transform of  $v_i(t)$ , and the following equation can be derived:

$$V_{ref,i}(s) = V_i(s) \quad (23)$$

Substituting (21) and (23) into (22), we can obtain:

$$sV_i(s) = v_{nom} - sI_{pu,i}(s)m + (sk_{pv} + k_{iv}) \left( \frac{v_{nom}}{s} - V_{ave,i}(s) \right) - (sk_{pc} + k_{ic}) \sum_{j \in \{i, N_i\}} w_{i,j} I_{pu,j}(s) \quad (24)$$

By multiplying both sides of the above equation by  $s$  and rewriting it in the compact form, the following equation can be derived:

$$s^2\mathbf{V}(s) = s\mathbf{v}_{nom} - s^2\mathbf{I}_{pu}(s)m + (sk_{pv} + k_{iv})(\mathbf{v}_{nom} - s\mathbf{V}_{ave}(s)) - (sk_{pc} + k_{ic})\mathbf{W}s\mathbf{I}_{pu}(s) \quad (25)$$

where  $\mathbf{V}(s) = [V_1(s), V_2(s), \dots, V_n(s)]^T$ ;  $\mathbf{v}_{nom} = [v_{nom}, v_{nom}, \dots, v_{nom}]^T$ ;  $\mathbf{I}_{pu}(s) = [I_{pu,1}(s), I_{pu,2}(s), \dots, I_{pu,n}(s)]^T$ ; and  $\mathbf{V}_{ave}(s) = [V_{ave,1}(s), V_{ave,2}(s), \dots, V_{ave,n}(s)]^T$ .

Define  $i_{pu,i}^{ss}$  as the output per-unit current of DG  $i$  in the steady state, and  $\mathbf{i}_{pu}^{ss} = [i_{pu,1}^{ss}, i_{pu,2}^{ss}, \dots, i_{pu,n}^{ss}]^T$ . Thus, according to the final value theory of Laplace transform, we can obtain:

$$\mathbf{i}_{pu}^{ss} = \lim_{s \rightarrow 0} s \mathbf{I}_{pu}(s) \quad (26)$$

Based on the final value theorem [34] and substituting (18) and (26) into the limit form of (25), we can obtain:

$$\begin{aligned} \lim_{s \rightarrow 0} s^2 \mathbf{V}(s) &= \lim_{s \rightarrow 0} \left\{ s \mathbf{v}_{nom} - s^2 \mathbf{I}_{pu}(s) \mathbf{m} + \right. \\ &\quad \left. (s k_{pv} + k_{iv})(\mathbf{v}_{nom} - s \mathbf{V}_{ave}(s)) - (s k_{pc} + k_{ic}) \mathbf{W} s \mathbf{I}_{pu}(s) \right\} \Rightarrow \\ \lim_{s \rightarrow 0} s \mathbf{v}^{ss} &= \lim_{s \rightarrow 0} \left\{ 0 - s \mathbf{i}_{pu}^{ss} \mathbf{m} + (0 + k_{iv})(\mathbf{v}_{nom} - \mathbf{v}^{ss}_{ave}) - \right. \\ &\quad \left. (0 + k_{ic}) \mathbf{W} \mathbf{i}_{pu}^{ss} \right\} \Rightarrow k_{ic} \mathbf{W} \mathbf{i}_{pu}^{ss} = k_{iv} \left\{ \mathbf{v}_{nom} - \mathbf{v}^{ss}_{ave} \right\} \end{aligned} \quad (27)$$

Comparing (27) and Property 2 shown in (8), we can conclude that the average bus voltage obtained by each DG agent via the distributed discovery algorithm can converge to the nominal value and the current can be proportionally dispatched among DGs in the steady state. Thus, the proposed control objectives presented in Section III-A can be satisfied with the proposed secondary control.

Figure 2 presents the schematic diagram of distributed secondary control. The primary droop controllers are generally with much higher response speed than the distributed secondary controller. Furthermore, the time frame of the primary droop control is generally between 0.1 ms and 10 ms [33], and the time frame of the distributed secondary control is generally between 100 ms and 1 s [35]. Thus, the sampling as well as communication interval is designed as 10 ms for the distributed secondary control, which can provide an adequate tradeoff between the response speed and communication burden of the distributed secondary control. As shown in Fig. 2, a memory block is applied to store the information received from its neighboring agents by communicating with its neighboring agents, and the period is fixed to be 10 ms.

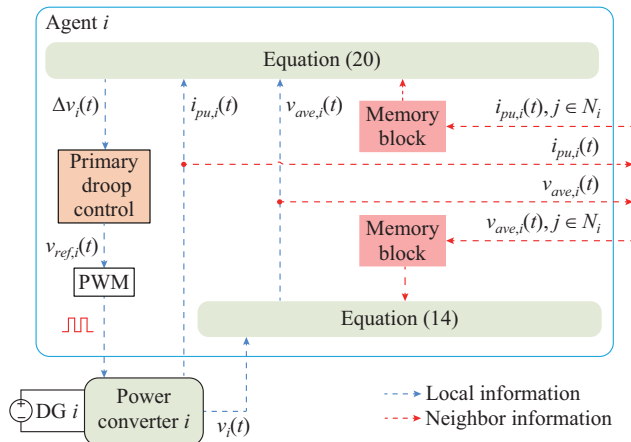


Fig. 2. Schematic diagram of distributed secondary control.

#### IV. EVENT-TRIGGERED IMPLEMENTATION OF PROPOSED SECONDARY CONTROL

In this section, the event-triggered communication strategy is first designed. Then, the convergence analysis of the

event-triggered secondary control is presented.

##### A. Event-triggered Communication Strategy

In order to implement the distributed average bus voltage discovery algorithm shown in (14) and the distributed secondary control algorithm shown in (20), the information about the discovered average bus voltage  $v_{ave,i}$  and the output per-unit current  $i_{pu,i}$  acquired by the  $i^{\text{th}}$  agent need to be exchanged by communicating with neighboring agents. The communication could be achieved in a time-triggered strategy or an event-triggered strategy. For the time-triggered strategy, communication is executed in a fixed sampling or control period, which will cause many cases of redundant communication [18]. For the event-triggered strategy, communication will be executed only when the state is triggered by certain event. To reduce the communication burdens, an event-triggered condition is designed as shown in Fig. 3 and (28).

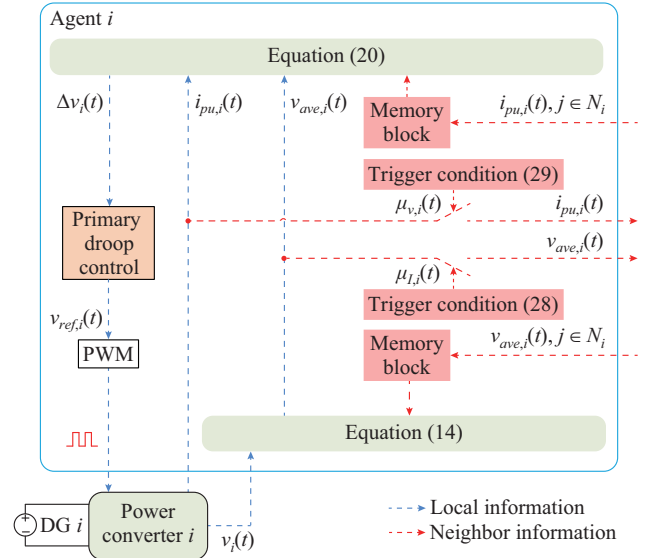


Fig. 3. Schematic diagram of event-triggered secondary control.

$$\mu_{v,i}(t) = \begin{cases} 1 & |v_{ave,i}(t) - v_{ave,i}(t - T_s)| > \beta v_{nom} \\ 0 & \text{otherwise} \end{cases} \quad (28)$$

where  $\mu_{v,i}(t)$  is the communication state to exchange the discovered average bus voltage  $v_{ave,i}$  with neighboring agents;  $\beta$  is the permissible error threshold; and  $T_s$  is the sampling and minimum communication interval of the proposed secondary control, which is set as 10 ms, as presented in Section III-C. Thus, the time interval between two event-triggered instances is at least lower bounded by the constant sampling interval  $T_s = 10$  ms, which ensures that Zeno-behavior is excluded.

When the event is triggered, i. e.,  $\mu_{v,i}(t) = 1$ , the variable  $v_{ave,i}$  needs to transfer to its neighbors through communication and then the neighboring agents will update their memories with the newly-updated variable  $v_{ave,i}$  as shown in Fig. 3. Otherwise, i. e.,  $\mu_{v,i}(t) = 0$ , the communication is avoided in this control period and the algorithm shown in (14) will be executed with the corresponding value that is stored in the

memory.

For the distributed secondary control shown in (20), the event-triggered condition is designed as:

$$\mu_{l,i}(t) = \begin{cases} 1 & |i_{pu,i}(t) - i_{pu,i}(t - T_s)| > \beta i_{pu,i}(t) \\ 0 & \text{otherwise} \end{cases} \quad (29)$$

where  $\mu_{l,i}(t)$  is the communication state to exchange the output per-unit current  $i_{pu,i}$  between neighboring agents.

When the event is triggered, i.e.,  $\mu_{l,i}(t)=1$ , the variable  $i_{pu,i}(t)$  needs to be transferred to its neighbors through communication and then the neighboring agents will update their memories with the newly-updated variable  $i_{pu,i}(t)$  as shown in Fig. 3. Otherwise, i.e.,  $\mu_{l,i}(t)=0$ , the communication is avoided in this control period and the algorithm shown in (20) will be executed with the corresponding value stored in the memory.

As shown in Fig. 3, only the local measured information, i.e.,  $v_{ave,i}$  and  $i_{pu,i}$ , are required to generate the event-triggered condition. However, for those methods proposed in [16], [17], certain state estimators are required to generate event-triggered condition. While the proposed event-triggered method shows lower computation burden and is easier to implement. In addition, as shown in (28) and (29), only the permissible error threshold  $\beta$  needs to be designed for the event-triggered condition. However, for the methods proposed in [19], [20], several parameters and a positive definite matrix need to be well designed for event-triggered condition. Thus, the proposed secondary control is easier to implement.

### B. Convergence Analysis

Different from the convergence analysis of the proposed secondary control under the time-triggered communication mechanism shown in Section III, the convergence of a distributed control strategy under the event-triggered communication mechanism generally needs to be further evaluated [36]. In order to analyze the convergence of the event-triggered communication mechanism shown in (28) and (29),  $\mu_{v,i}^{ss}$  and  $\mu_{l,i}^{ss}$  are defined as the steady-state values of  $\mu_{v,i}(t)$  and  $\mu_{l,i}(t)$ , respectively. According to (28) and (29), the convergence of the proposed event-triggered secondary control is related to  $\mu_{v,i}(t)$  and  $\mu_{l,i}(t)$ .

The convergence of the event-triggered communication mechanism shown in (28) can be proven based on the following two cases.

1) All the agents satisfy  $\mu_{v,i}^{ss}=1$ . In this case, the event-triggered control strategy degrades into a time-triggered strategy. Based on the convergence analysis presented in Section III, the algorithms shown by (14) is converged when they are implemented with the time-triggered strategy. Thus, this case is impossible because the assumption of  $\mu_{v,i}^{ss}=1$  is invalid during the converging process.

2) At least one agent satisfies  $\mu_{v,i}^{ss}=0$ . For the proposed average bus voltage discovery algorithm shown in (14), the stability analysis is as follows: ① according to (28),  $v_{ave,i}^{ss}$  will converge to a certain value with acceptable small variation if  $\beta$  is small enough; ② furthermore, according to (14), if the discovered average bus voltage  $v_{ave,i}^{ss}$  of the other DGs have

big differences, then  $v_{ave,i}^{ss}$  will fluctuate widely that makes the assumption of  $\mu_{v,i}^{ss}=0$  invalid according to the distributed consensus theory. Thus, the discovered average bus voltage will be converged if  $\beta$  is small enough.

The convergence of the event-triggered mechanism shown in (29) can also be proven based on the following two cases.

1) All the agents satisfy  $\mu_{l,i}^{ss}=1$ . In this case, the event-triggered control strategy degrades into a time-triggered strategy. Based on the convergence analysis presented in Section III, the algorithm shown in (20) is converged when it is implemented with the time-triggered strategy. Thus, this case is impossible because the assumption of  $\mu_{l,i}^{ss}=1$  is invalid during the converging process.

2) At least one agent satisfies  $\mu_{l,i}^{ss}=0$ . For the proposed secondary control shown in (20), the stability analysis is as follows: ① according to (29),  $i_{pu,i}^{ss}$  will converge to a certain value with acceptable small variation if  $\beta$  is small enough; ② furthermore, according to (20), if the output per-unit currents  $i_{pu,i}^{ss}$  of the other DGs have big differences, then according to distributed consensus theory,  $\Delta v_i^{ss}$  will fluctuate widely, which will cause a large fluctuation of  $i_{pu,i}^{ss}$  and make the assumption of  $\mu_{l,i}^{ss}=0$  invalid. Thus, the proposed secondary control strategy will also converge if  $\beta$  is small enough.

## V. SIMULATION VERIFICATION AND RESULT ANALYSIS

To evaluate the performance of the proposed event-triggered secondary control, a DC microgrid shown in Fig. 4 is simulated in MATLAB/SimPowerSystems.

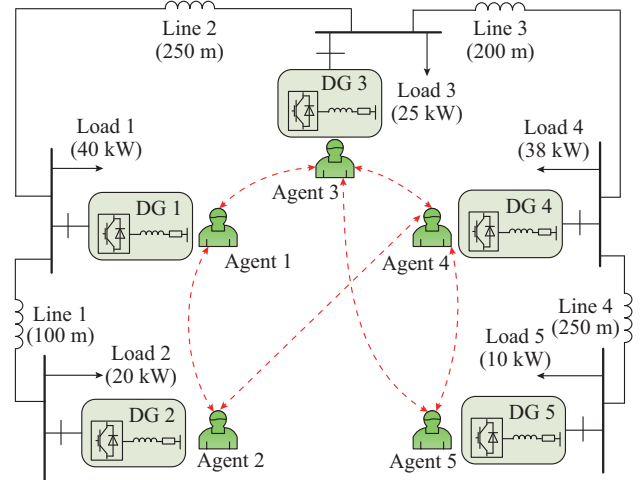


Fig. 4. Structure of DC microgrid test system.

As shown in Fig. 4, the studied DC microgrid contains five DGs, and each DG is assigned with an agent that can communicate with its neighbors. The nominal DC bus voltage is 400 V. The length of each transmission line and the load demand in each bus are also shown in Fig. 4. The resistance of the transmission lines in the DC microgrid is set as  $0.325 \Omega/\text{km}$  [37]. In this paper, in order to improve the robustness of the proposed control strategy, the communication topology of the agents is designed to satisfy the  $N-1$  rule [38], which will assure that any two agents in the communication network remain connected in case of a communica-

tion link fault. The detailed parameters of the DGs and the communication topology of the agents are shown in Table I. The maximum admissible voltage droop is generally designed as percentage of the nominal DC bus voltage [39], thus the droop coefficient  $m$  is set as  $5\% \times 400 \text{ V} = 20 \text{ V}$  in this paper. According to the proportional-integral (PI) tuning rules [40], the parameters of  $\varepsilon$ ,  $k_{pv}$ ,  $k_{iv}$ ,  $k_{pc}$ , and  $k_{ic}$  shown in (14) and (20) are set as 10, 0.05, 12, 5, and 600, respectively, which can give a good tradeoff between overshoot and response speed. In order to improve the performance of the proposed control method, the above parameters can also be offline optimized by certain artificial intelligence (AI)-based algorithms, such as particle swarm optimization [41], ant colony optimization [42], and genetic algorithm [43]. However, this paper intends to ensure the average bus voltage regulation and proportional load sharing of a DC microgrid through designing an event-triggered secondary control strategy. The AI-based parameter optimization will be considered in our future work.

TABLE I  
PARAMETERS OF DGs AND AGENTS

Index of DG	Neighboring agents	Capacity (kW)
1	2, 3	60
2	1, 4	24
3	1, 4, 5	40
4	2, 3, 5	30
5	3, 4	35

#### A. Verification of Proposed Secondary Control in Case of Time-triggered Strategy

The performance of proposed secondary control is firstly verified in case of time-triggered method. It should be noted that the event-triggered method will degrade into time-triggered method when permissible error threshold in (28) and (29) is set as  $\beta=0$ . In time-triggered method, the periodic communication between neighboring agents is conducted in a fixed time interval of 10 ms as shown in Section III-C. For this case, the corresponding scenarios are designed as: ① before  $t=2$  s, only the primary droop control is enabled; ② during  $t=2$  s to  $t=6$  s, only the average bus voltage discovery algorithm is enabled; ③ after  $t=6$  s, the proposed secondary control is started to regulate the average bus voltage and ensure proportional current sharing.

In terms of the time-triggered method, the performance of proposed secondary control is shown in Fig. 5.

Before  $t=2$  s, the average bus voltage of each DG is set with its local measured voltage value, as shown in Fig. 5(a). When the distributed average bus voltage discovery algorithm is enabled after  $t=2$  s, the discovered average bus voltage of each DG can converges to real average bus voltage within a short transient process. Before  $t=6$  s, the currents are shared based on the primary droop control. When the proposed secondary control is enabled after  $t=6$  s, the average bus voltage can be regulated to its nominal value, i.e., 400 V, as shown in Fig. 5(a), and the current of each DG can be shared in proportion to their capacities, as shown in

Fig. 5(b). Thus, the proposed secondary control can satisfy both of the control objectives presented in Section III-A, and shows good transient and steady-state performances.

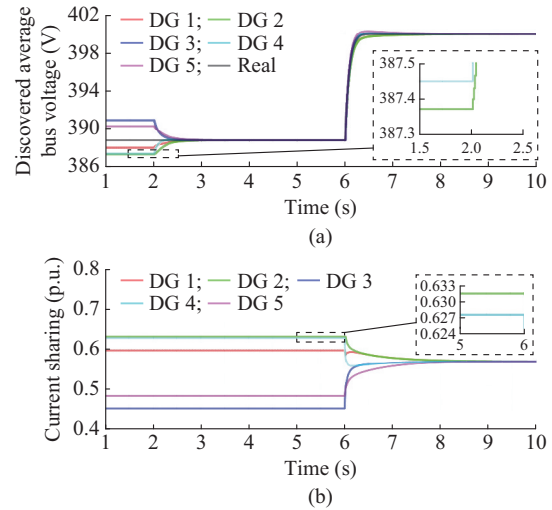


Fig. 5. Performance of proposed secondary control in case of time-triggered strategy. (a) Average bus voltage. (b) Current sharing of each DG.

#### B. Verification of Proposed Secondary Control in Case of Event-triggered Strategy

It should be noted that the permissible error threshold  $\beta$  in (28) and (29) affects both the control accuracy and the communication burden of the proposed secondary control. To verify the performance of the proposed secondary control, the performance comparison of the proposed secondary control is carried out using six different  $\beta$  values as shown in Fig. 6. Other conditions are the same as those used in Fig. 5.

The event-triggered method will degrade into the time-triggered strategy in case of  $\beta=0$ . As demonstrated in Fig. 5, the time-triggered method, i.e.,  $\beta=0$ , shows good transient and steady-state performances. Thus, the results of the event-triggered strategy in terms of  $\beta=0$  can be taken as a benchmark. As shown in Fig. 6(a) and (b), with the increase of  $\beta$ , both the discovered average bus voltage and the current sharing show higher deviations from those shown in the benchmark case, i.e.,  $\beta=0$  in the steady-state. Figure 6(c) and (d) demonstrates the event-triggering time sequences of  $\mu_{v,1}(t)$  and  $\mu_{i,1}(t)$  using six different  $\beta$  values, respectively. In Fig. 6(c) and (d), the vertical axis labels of 1-6 represent case indexes associated with  $\beta$  values of 0,  $0.5 \times 10^{-5}$ ,  $1 \times 10^{-5}$ ,  $1.5 \times 10^{-5}$ ,  $2 \times 10^{-5}$ , and  $2.5 \times 10^{-5}$ , respectively. The “|” symbol in Fig. 6(c) and (d) represent that the corresponding event-triggered condition is satisfied, and communication is needed to exchange data between neighboring agents. Figure 6(e) and (f) demonstrates the number of communication events required to exchange  $v_{ave,i}$  and  $i_{pu,i}$  among neighboring agents, respectively, under different  $\beta$  values during  $t=6-10$  s. As shown in Fig. 6(c) - (e), the communication burden is increased with the decrease of  $\beta$  values. Based on the analysis,  $\beta$  is set as  $1 \times 10^{-5}$ , which can give a proper trade-off between the control accuracy and the communication burden of the proposed control strategy.

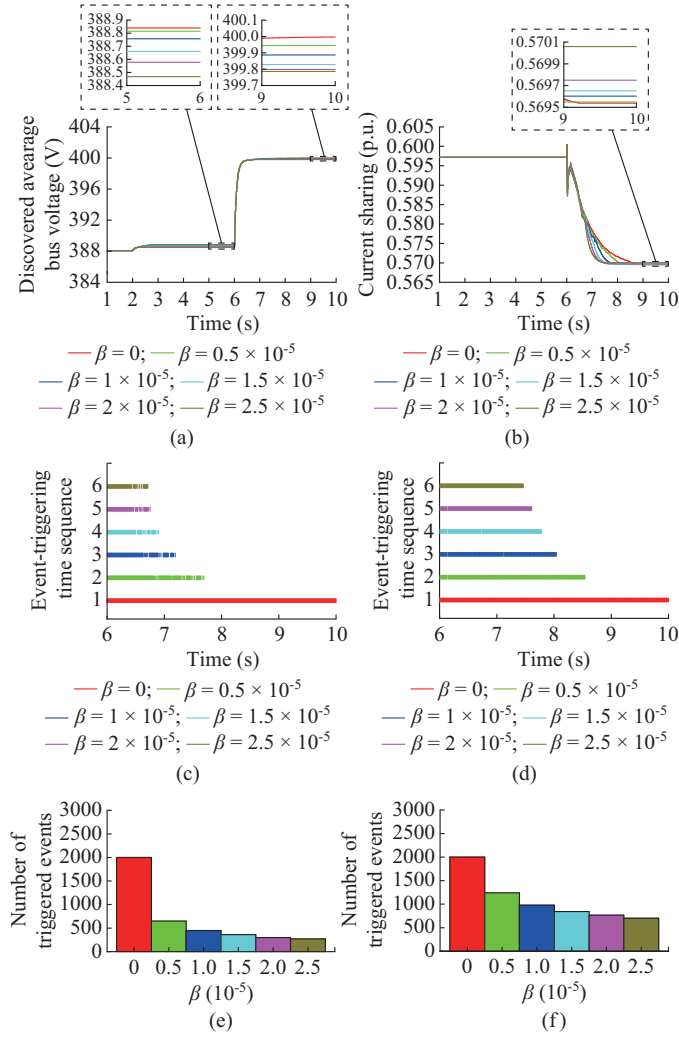


Fig. 6. Performance comparison of proposed secondary control with different  $\beta$  values in case of event-triggered strategy. (a) Average bus voltage discovered by agent 1 with different  $\beta$  values. (b) Current sharing of DG 1 with different  $\beta$  values. (c) Event-triggering time sequences of  $\mu_{v,1}(t)$  with different  $\beta$  values. (d) Event-triggering time sequences of  $\mu_{l,1}(t)$  with different  $\beta$  values. (e) Number of triggered events required to exchange data  $v_{ave,i}$  among neighboring agents with different  $\beta$  values during  $t=6-10$  s. (f) Number of triggered events required to exchange data  $i_{pu,i}$  among neighboring agents with different  $\beta$  values during  $t=6-10$  s.

### C. Verification of Proposed Secondary Control Under Over-load Conditions

In order to verify the performance of the proposed event-triggered secondary control under over-load conditions, the scenarios are set as follows: ① all the load demands are increased to 1.7 times of that presented in Fig. 4; ② before  $t=3$  s, the current limitations are not considered; ③ after  $t=3$  s, under over-current conditions, the over-currents of DGs are limited by generating additional voltage regulation terms that drive the corresponding DGs operating under their maximum allowable currents; ④ after  $t=6$  s, the proposed event-triggered secondary control is enabled to regulate the average bus voltage and ensure the proportional current sharing.

Figure 7 presents a performance evaluation of the proposed secondary control under over-load conditions.

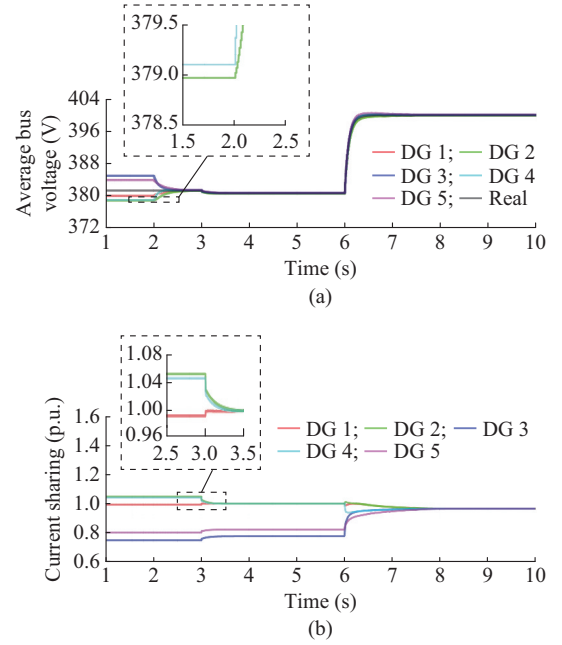


Fig. 7. Performance evaluation of proposed secondary control under over-load conditions. (a) Average bus voltage. (b) Current sharing of each DG.

As shown in Fig. 7, before  $t=3$  s, DG 2 and DG 4 are over-loaded, and their currents are higher than 1 p.u.. After  $t=3$  s, the current limitation strategy is enabled, thus, the currents of DG 2 and DG 4 are reduced to 1 p.u., and the currents of the rest DGs are increased to meet the load demand. Especially, the current of DG 1 is also limited to 1 p.u. during  $t=3-6$  s. After  $t=6$  s, the average bus voltage is regulated to its nominal value and the current of each DG is shared in proportional to their capacities, which demonstrates the effectiveness of the proposed secondary control even under over-load conditions.

### D. Verification of Proposed Secondary Control in Case of Load Variation

To verify the performance of the proposed event-triggered secondary control in the case of a load variation, a case study has been conducted using the following scenarios: ① before  $t=10$  s, load 3 is turned off and all the other loads are turned on; ② at  $t=10$  s, load 4 is turned off; ③ at  $t=14$  s, load 4 is turned on again; ④ at  $t=18$  s, load 3 is turned on; ⑤ at  $t=22$  s, load 3 is turned off.

The performance evaluation of the proposed secondary control in case of the load variation is shown in Fig. 8. In this case, the average bus voltage can be restored to the nominal value, i.e., 400 V, with an admissible short-term transient process.

As shown in Fig. 8(b) and (c), in case of the load variation, the generated power and output current can be proportionally dispatched among the DGs with a short-term transient. Thus, the proposed secondary control can satisfy the control objectives presented in Section III-A, and shows good transient and steady-state performances in case of load variation.

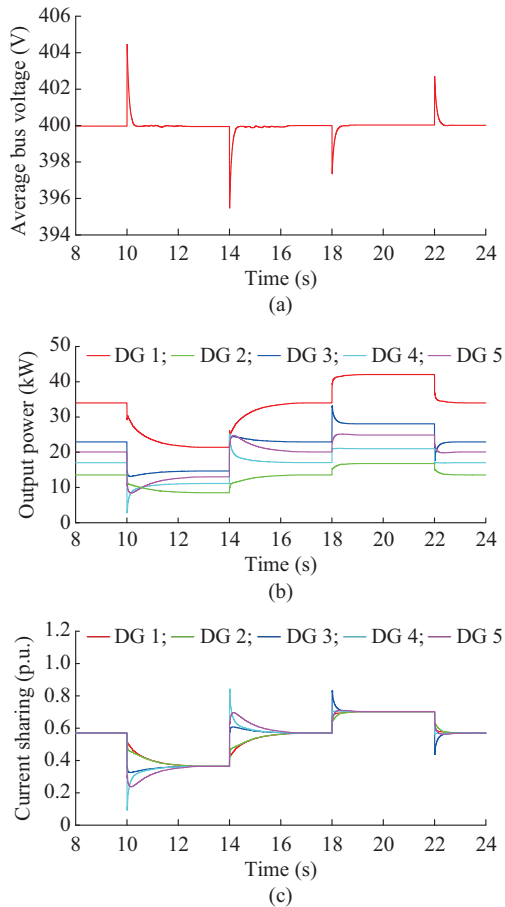


Fig. 8. Performance evaluation of proposed secondary control in case of load variation. (a) Average bus voltage of DC microgrid. (b) Output power of each DG. (c) Current sharing of each DG.

### E. Robustness Evaluation in Case of Plug-and-play and Agent Loss

In order to verify the performance of the proposed secondary control in handling the plug-and-play requirement and agent loss, a case study has been conducted using the following scenarios: ① during  $t=26-30$  s, DG 5 is turned off, and its corresponding agent (agent 5) is also shut down; ② after  $t=30$  s, DG 5 and agent 5 are turned on again; ③ during  $t=34-38$  s, agent 5 is lost and load 4 is turned off, and DG 5 is disconnected from the microgrid; ④ after  $t=38$  s, agent 5 is recovered and DG 5 is turned on again.

As shown in Fig. 9(a), based on the updated multi-agent system that consists of agents 1-4, the average voltage can restore to its nominal value in cases of the shutdown of DG 5 and the loss of agent 5 during  $t=26-30$  s and  $t=34-38$  s.

When agent 5 is lost during  $t=34-38$  s, it loses the communication link with the rest agents. However, the matrix  $W$  can be updated based on the updated communication topology of the rest agents. Thus, as shown in Fig. 9(c), during  $t=34-38$  s, the other DGs can still ensure a proportional current sharing. In conclusion, as shown in Fig. 9, the proposed secondary control shows good robustness in handling the plug-and-play and agent loss.

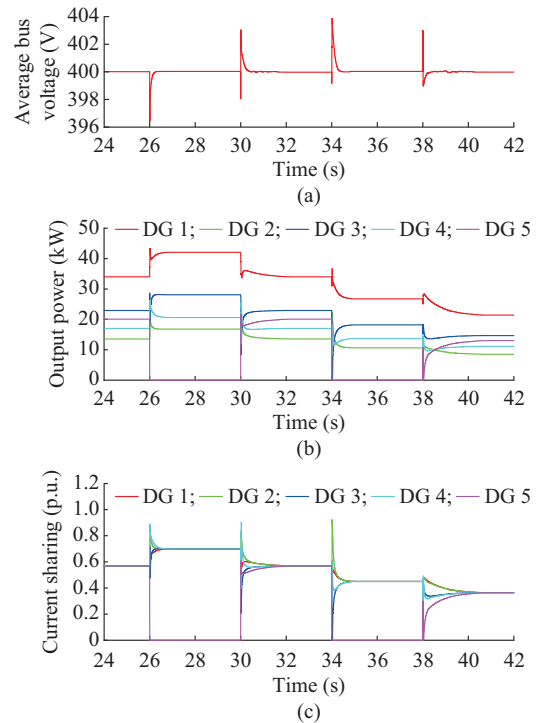


Fig. 9. Robustness evaluation of proposed secondary control in case of plug-and-play and agent loss. (a) Average bus voltage of DC microgrid. (b) Output power of each DG. (c) Current sharing of each DG.

## VI. CONCLUSION

A distributed and event-triggered secondary control is proposed to ensure the average bus voltage restoration and proportional current sharing for DC microgrid. An event-triggered condition is also designed to reduce the communication burden among the neighboring agents, which does not need extra state estimators and is easy to implement. The proposed control method also shows good robustness against load variation, plug-and-play, and agent faults. For future work, we plan to investigate the potential to extend the proposed secondary control to voltage and frequency regulation for AC and hybrid AC/DC microgrids. Besides, the improved control strategy and detailed analysis of time delays on the performance of the proposed secondary control are also the future research plans.

## REFERENCES

- [1] F. Gao, R. Kang, J. Cao *et al.*, "Primary and secondary control in DC microgrids: a review," *Journal of Modern Power Systems and Clean Energy*, vol. 7, no. 2, pp. 227-242, Mar. 2019.
- [2] Z. Cheng, Z. Li, S. Li *et al.*, "A novel cascaded control to improve stability and inertia of parallel buck-boost converters in DC microgrid," *International Journal of Electrical Power & Energy Systems*, vol. 119, p. 105950, Jul. 2020.
- [3] H. Liu, Y. Wang, M. Wang *et al.*, "Small-signal analysis of DC microgrid and multi-objective optimization segmented droop control suitable for economic dispatch," *Journal of Modern Power Systems and Clean Energy*, vol. 8, no. 3, pp. 564-572, May 2020.
- [4] J. M. Guerrero, J. C. Vasquez, J. Matas *et al.*, "Hierarchical control of droop-controlled AC and DC microgrids—a general approach toward standardization," *IEEE Transactions on Industrial Electronics*, vol. 58, no. 1, pp. 158-172, Jan. 2011.
- [5] Z. Shuai, J. Fang, F. Ning *et al.*, "Hierarchical structure and bus voltage control of DC microgrid," *Renewable & Sustainable Energy Reviews*, vol. 82, pp. 3670-3682, Feb. 2018.

- [6] M. Yuan, Y. Fu, Y. Mi *et al.*, "Hierarchical control of DC microgrid with dynamical load power sharing," *Applied Energy*, vol. 239, pp. 1-11, Apr. 2019.
- [7] H. Kakigano, Y. Miura, and T. Ise, "Distribution voltage control for DC microgrids using fuzzy control and gain-scheduling technique," *IEEE Transactions on Power Electronics*, vol. 28, no. 5, pp. 2246-2258, May 2013.
- [8] Z. Li, C. Zang, P. Zeng *et al.*, "Fully distributed hierarchical control of parallel grid-supporting inverters in islanded AC microgrids," *IEEE Transactions on Industrial Informatics*, vol. 14, no. 2, pp. 679-690, Feb. 2018.
- [9] S. Anand, B. G. Fernandes, and J. Guerrero, "Distributed control to ensure proportional load sharing and improve voltage regulation in low-voltage DC microgrids," *IEEE Transactions on Power Electronics*, vol. 28, no. 4, pp. 1900-1913, Apr. 2013.
- [10] P. Huang, P. Liu, W. Xiao *et al.*, "A novel droop-based average voltage sharing control strategy for DC microgrids," *IEEE Transactions on Smart Grid*, vol. 6, no. 3, pp. 1096-1106, May 2015.
- [11] X. Lu, J. M. Guerrero, K. Sun *et al.*, "An improved droop control method for DC microgrids based on low bandwidth communication with DC bus voltage restoration and enhanced current sharing accuracy," *IEEE Transactions on Power Electronics*, vol. 29, no. 4, pp. 1800-1812, Apr. 2014.
- [12] P. Wang, X. Lu, X. Yang *et al.*, "An improved distributed secondary control method for DC microgrids with enhanced dynamic current sharing performance," *IEEE Transactions on Power Electronics*, vol. 31, no. 9, pp. 6658-6673, Sept. 2016.
- [13] L. Ding, Q. Han, L. Y. Wang *et al.*, "Distributed cooperative optimal control of DC microgrids with communication delays," *IEEE Transactions on Industrial Informatics*, vol. 14, no. 9, pp. 3924-3935, Sept. 2018.
- [14] A. Nawaz, J. Wu, and C. Long, "Mitigation of circulating currents for proportional current sharing and voltage stability of isolated DC microgrid," *Electric Power Systems Research*, vol. 180, p. 106123, Mar. 2020.
- [15] D. Dam and H. Lee, "A power distributed control method for proportional load power sharing and bus voltage restoration in a DC microgrid," *IEEE Transactions on Industry Applications*, vol. 54, no. 4, pp. 3616-3625, July 2018.
- [16] S. Sahoo and S. Mishra, "An adaptive event-triggered communication-based distributed secondary control for DC microgrids," *IEEE Transactions on Smart Grid*, vol. 9, no. 6, pp. 6674-6683, Nov. 2018.
- [17] D. Pullaguram, S. Mishra, and N. Senroy, "Event-triggered communication based distributed control scheme for DC microgrid," *IEEE Transactions on Power Systems*, vol. 33, no. 5, pp. 5583-5593, Sept. 2018.
- [18] R. Han, L. Meng, J. M. Guerrero *et al.*, "Distributed nonlinear control with event-triggered communication to achieve current-sharing and voltage regulation in DC microgrids," *IEEE Transactions on Power Electronics*, vol. 33, no. 7, pp. 6416-6433, Jul. 2018.
- [19] B. Fan, J. Peng, Q. Yang *et al.*, "Distributed periodic event-triggered algorithm for current sharing and voltage regulation in DC microgrids," *IEEE Transactions on Smart Grid*, vol. 11, no. 1, pp. 577-589, Jan. 2020.
- [20] F. Guo, L. Wang, C. Wen *et al.*, "Distributed voltage restoration and current sharing control in islanded DC microgrid systems without continuous communication," *IEEE Transactions on Industrial Electronics*, vol. 67, no. 4, pp. 3043-3053, Apr. 2020.
- [21] S. Kar and J. M. F. Moura, "Distributed consensus algorithms in sensor networks: quantized data and random link failures," *IEEE Transactions on Signal Processing*, vol. 58, no. 3, pp. 1383-1400, Mar. 2010.
- [22] Y. Xu, W. Zhang, and W. Liu, "Distributed dynamic programming-based approach for economic dispatch in smart grids," *IEEE Transactions on Industrial Informatics*, vol. 11, no. 1, pp. 166-175, Feb. 2015.
- [23] W. Ren, R. W. Beard, and E. M. Atkins, "A survey of consensus problems in multi-agent coordination," in *Proceedings of 2005 American Control Conference*, Portland, USA, Jun. 2005, pp. 1859-1864.
- [24] R. Olfati-Saber, J. A. Fax, and R. M. Murray, "Consensus and cooperation in networked multi-agent systems," *Proceedings of the IEEE*, vol. 95, no. 1, pp. 215-233, Jan. 2007.
- [25] R. Olfati-Saber and R. M. Murray, "Consensus problems in networks of agents with switching topology and time-delays," *IEEE Transactions on Automatic Control*, vol. 49, no. 9, pp. 1520-1533, Sept. 2004.
- [26] C. D. Meyer, *Matrix Analysis and Applied Linear Algebra*, Philadelphia: SIAM Press, 2000.
- [27] A. D. Porter, "Solvability of the matrix equation  $AX=B$ ," *Linear Algebra and Its Applications*, vol. 13, no. 3, pp. 177-184, Mar. 1976.
- [28] C. Papadimitriou, E. Zountouridou, and N. Hatziaargyriou, "Review of hierarchical control in DC microgrids," *Electric Power Systems Research*, vol. 122, pp. 159-167, May 2015.
- [29] Q. Shafiee, T. Dragicevic, J. C. Vasquez *et al.*, "Hierarchical control for multiple DC-microgrids clusters," *IEEE Transactions on Energy Conversion*, vol. 29, pp. 922-933, Dec. 2014.
- [30] V. Nasirian, A. Davoudi, and F. L. Lewis, "Distributed adaptive droop control for DC microgrids," in *Proceedings of 2014 IEEE Applied Power Electronics Conference and Exposition*, Fort Worth, USA, pp. 1147-1152, Mar. 2014.
- [31] V. Nasirian, S. Moayedi, A. Davoudi *et al.*, "Distributed cooperative control of DC microgrids," *IEEE Transactions on Power Electronics*, vol. 30, no. 4, pp. 2288-2303, Apr. 2015.
- [32] S. Sahoo and S. Mishra, "A distributed finite-time secondary average voltage regulation and current sharing controller for DC microgrids," *IEEE Transactions on Smart Grid*, vol. 10, no. 1, pp. 282-292, Jan. 2019.
- [33] X. Feng, A. Shekhar, F. Yang *et al.*, "Comparison of hierarchical control and distributed control for microgrid," *Electric Power Components and Systems*, vol. 45, no. 10, pp. 1043-1056, Oct. 2017.
- [34] R. C. Dorf and R. H. Bishop, *Modern Control Systems*, Upper Saddle River: Prentice Hall, 2011.
- [35] G. Messinis, F. Gonzalez-Espin, V. Valdivia *et al.*, "Application of rapid prototyping tools for a hierarchical microgrid control implementation," in *Proceedings of 2014 IEEE 5th International Symposium on Power Electronics for Distributed Generation Systems*, Galway, Ireland, Jun. 2014, pp. 1-5.
- [36] L. Ding, Q. Han, and X. Zhang, "Distributed secondary control for active power sharing and frequency regulation in islanded microgrids using an event-triggered communication mechanism," *IEEE Transactions on Industrial Informatics*, vol. 15, no. 7, pp. 3910-3922, Jul. 2019.
- [37] N. Jayawarna and M. Barnes, "Study of a microgrid with vehicle-to-grid sources during network contingencies," *Intelligent Automation & Soft Computing*, vol. 16, no. 2, pp. 289-302, Mar. 2010.
- [38] W. Zhang, W. Liu, C. Zang *et al.*, "Multiagent system-based integrated solution for topology identification and state estimation," *IEEE Transactions on Industrial Informatics*, vol. 13, no. 2, pp. 714-724, Apr. 2017.
- [39] I. Cvetkovic, D. Dong, W. Zhang *et al.*, "A testbed for experimental validation of a low-voltage DC nanogrid for buildings," in *Proceedings of 2012 15th International Power Electronics and Motion Control Conference*, Novi Sad, Serbia, Sept. 2012, pp. 1-8.
- [40] A. O'Dwyer, "PI and PID controller tuning rules: an overview and personal perspective," in *Proceedings of 2006 IET Irish Signals and Systems Conference*, Dublin, Ireland, Jun. 2006, pp. 161-166.
- [41] M. Sharafi and T. Y. El Mekkawy, "Multi-objective optimal design of hybrid renewable energy systems using PSO-simulation based approach," *Renewable Energy*, vol. 68, pp. 67-79, Aug. 2014.
- [42] F. Zheng, A. C. Zecchin, J. P. Newman *et al.*, "An adaptive convergence-trajectory controlled ant colony optimization algorithm with application to water distribution system design problems," *IEEE Transactions on Evolutionary Computation*, vol. 21, pp. 773-791, Oct. 2017.
- [43] A. B. H. Adamou-Mitiche and L. Mitiche, "Multivariable systems model reduction based on the dominant modes and genetic algorithm," *IEEE Transactions on Industrial Electronics*, vol. 64, no. 2, pp. 1617-1619, Feb. 2017.

**Zhongwen Li** received the B.S. degree in control science and engineering from Zhengzhou University, Zhengzhou, China, in 2011, and the Ph.D. degree in control theory and control engineering from Shenyang Institute of Automation, Chinese Academy of Sciences, Shenyang, China, in 2017. He is currently an Associate Professor at the School of Electrical Engineering, Zhengzhou University. His main research interests include distributed control, multi-agent system, power electronics, power systems, renewable energy systems, PV generation system, and microgrids.

**Zhiping Cheng** received the B.S. degree in School of Physics Electronic Engineering from Xinyang Normal University, Xinyang, China, in 1998, and the M.S. degree in electrical engineering from Henan Polytechnic University, Jiaozuo, China, in 2003. He is currently an Associate Professor at Zhengzhou University. His main research interests include the theory, application, and control of renewable energy systems and microgrids.

**Jikai Si** received the B.S. degree in electrical engineering and automation

from the Jiaozuo Institute of Technology, Jiaozuo, China, in 1998, the M.S. degree in electrical engineering from Henan Polytechnic University, Jiaozuo, China, in 2005, and the Ph.D. degree from the School of Information and Electrical Engineering, China University of Mining and Technology, Xuzhou, China, in 2008. He is currently a Professor at Zhengzhou University, Zhengzhou, China. His main research interests include the theory, application, and control of special motor and power electronics.

**Shuhui Li** received the B.S. and M.S. degrees in electrical engineering from Southwest Jiaotong University, Chengdu, China, in 1983 and 1988, respectively, and the Ph.D. degree in electrical engineering from Texas Tech University, Lubbock, USA, in 1999. He was with the School of Electrical

Engineering, Southwest Jiaotong University, from 1988 to 1995, where his fields of research interest included electrified railways, power electronics, power systems, and power system harmonics. From 1995 to 1999, he was engaged in research on wind power, artificial neural networks, and applications of massive parallel processing. He joined Texas A&M University, Kingsville, USA, as an Assistant Professor, in 1999, and became an Associate Professor in 2003. He joined the University of Alabama, Tuscaloosa, USA, as an Associate Professor, in 2006. His current research interests include renewable energy systems, power electronics, power systems, electric machines and drives, and applications of artificial neural networks in energy systems.